W. C. Hayes
Director,
Orthopaedic Biomechanics Laboratory,
Beth Israel Hospital and
Harvard Medical School,
Boston, Mass. 02215

J. D. Gran
Division of Applied Mechanics,
Stanford University,
Stanford, Calif. 94305

M. L. Nagurka
Doctoral Candidate,
Department of Mechanical Engineering,
Massachusetts Institute of Technology,
Cambridge, Mass. 02139

J. M. Feldman

C. Oatis

Department of Orthopaedic
Surgical Research,
University of Pennsylvania,
Philadelphia, Pa. 19104

Leg Motion Analysis During Gait by Multiaxial Accelerometry: Theoretical Foundations and Preliminary Validations

A theoretical formulation for studying limb motions and joint kinetics by multiaxial accelerometry is developed. The technique is designed to study the swing phase of human gait, modeling the lower leg as a rigid body. Major advantages of the approach are that acceleration information needed for the calculation of forces and moments is generated directly, and that the method automatically generates its own initial conditions. Results of validation experiments using both artificial and experimental data demonstrate that the method is theoretically valid, but that it taxes available instrumentation and requires further development before it can be applied in a clinical setting.

Introduction

Locomotion and other activities of daily living result in large forces across human joints. Since these forces have been implicated in joint degeneration and in the loosening of prosthetic joint replacements, there has long been an interest in the measurement or prediction of joint forces. Primarily, indirect methods have been used, with joint resultant forces and moments calculated given measured kinematic data and assumed inertia properties. The required kinematic data usually are obtained from cinematography, electrogoniometers, or from target tracking systems, all of which yield displacements of the limb segments versus time. To obtain the necessary velocities and accelerations, numerical differentiation is required. This process magnifies high-frequency noise and requires the use of filtering [1] or interpolation to obtain useful differentiated displacements [2, 3].

Because of these difficulties with indirect measurements, there have been a few attempts to measure joint resultant forces directly using instrumented prostheses [4–7]. For the hip, these instrumented prostheses have generally measured resultant joint forces consistently lower (by about 50 percent) than those calculated theoretically. These lower values from patients with instrumented prostheses may be caused by less energetic gait patterns compared to those occurring in normal subjects [8]. However, these differences between directly measured and theoretically predicted joint forces emphasize the need for improved methods for the measurement or prediction of joint resultant forces and moments.

An alternative approach to study the kinetics of articulating limbs is to use body-fixed accelerometers to measure accelerations directly. This approach is attractive since it avoids the errors inherent in the differentiation of displacement data and allows for the direct calculation of both inertial and active forces. Gage [9], Smidt, et al. [10], and Robinson, et al. [11] outlined methods to measure with three orthogonal accelerometers the linear acceleration of the center of gravity of the human body. However, these techniques are dependent on other methods to generate the necessary initial conditions.

Recently, investigators have re-examined the theoretical framework of the accelerometry approach. Morris [12] developed a theoretical analysis to describe three-dimensional motion using six accelerometers. Kane, et al. [13] presented a theory for a twelve-accelerometer approach, which was implemented experimentally to determine the forces exerted on a tennis racket during swing. Padganokar, et al. [14] showed that data reduction from Morris' six accelerometer scheme can be unreliable experimentally and extended the theoretical development based on nine linear accelerometers.

Contributed by the Bioengineering Division for publication in the JOURNAL OF BIOMECHANICAL ENGINEERING. Manuscript received by the Bioengineering Division, May 12, 1981; revised manuscript recived March 1, 1983.

Mital and King [15] pointed out that noncommutativity of finite rotations can lead to errors during numerical integration in the determination of the orientation of a rigid body. They suggested an alternative approach based on an orientation vector concept.

Multiaxial accelerometry represents a promising method to study limb motions and joint forces. This paper describes the theoretical formulation and preliminary experimental implementation of the accelerometry technique. The technique is designed to study the swing phase of human gait, modeling the lower leg as a rigid body. This approach offers three major advantages. First, acceleration information needed for the calculation of forces and moments is generated directly from the accelerometers during gait. Second, the method automatically generates its own initial conditions. Finally, given the availability of miniature accelerometers and computer-aided data acquisition, the method could be a viable clinical tool. Results of validation experiments using both artificial and experimental data demonstrate that the method is theoretically valid, but that it taxes available instrumentation and requires further development before it can be applied in a clinical setting.

Theoretical Formulation

This formulation was developed for studying the rigid-body motion of the lower leg during gait. The following parameters are determined from simultaneous triaxial accelerometer measurements on the leg: 1) the angular position, velocity and acceleration of the leg; 2) the linear position, velocity, and acceleration of the center of mass of the leg; 3) the resultant force and moment acting at the knee. The theoretical formulation requires the determination of the initial orientation of the leg. This initial condition is calculated by exploiting the following facts: 1) during the "foot-flat" cycle of gait, the motion of the leg is constrained; and 2) accelerometers measure components of gravity. Given the initial orientation obtained in the period of constrained motion during "foot-flat," the analysis then is applicable to all subsequent motion of the leg. This section discusses the analysis for time $t=0$ (involving the determination of the initial orientation during constrained motion), and then outlines the analysis for all subsequent time.

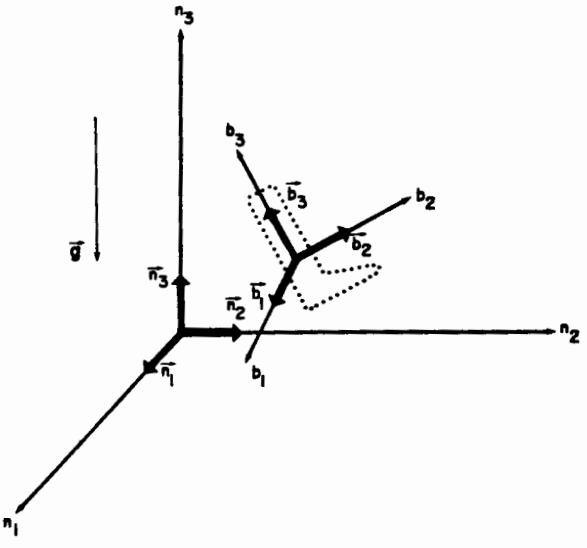

Fig. 1 Body-fixed and inertia-fixed reference frames, and associated unit vectors

Initial Conditions ($t=0$). Two orthogonal coordinate systems, inertial and body-fixed, are shown in Fig. 1. The n_i's denote an inertial reference frame, with associated unit vectors $\mathbf{n}_i$'s, orientated such that the directions of the gravity vector ($\mathbf{g}$) and the negative n_3 axis are the same. Similarly, the b_i's represent axes fixed in the leg, with corresponding unit vectors $\mathbf{b}_i$'s. The axes of this body-fixed frame coincide with the directions of the three principal mass moments of inertia, and the origin is located at the leg's center of mass. The orientation of the leg is specified relative to the inertial reference frame by three orientation angles, θ_1, θ_2, and θ_3. Body-fixed unit vectors ($\mathbf{b}_i$'s), initially aligned with the inertial frame unit vectors ($\mathbf{n}_i$'s), are rotated successively through angles θ_1, θ_2, and θ_3 to define the orientation of the leg.

To find orientation information, the development depends upon the fact that actual acceleration information of points on the leg is not available from accelerometry. A inertial-mass-type accelerometer consists of a semiconductor strain

Nomenclature

$\mathbf{a}$ = acceleration of center of mass of leg
$\mathbf{a}_i, i = 1, 2, 3, 4$ = acceleration at accelerometer location i
$\mathbf{a}_i^a, i = 1, 2, 3, 4$ = actual acceleration at accelerometer location i
$\mathbf{a}_i^m, i = 1, 2, 3, 4$ = measured acceleration at accelerometer location i
$\mathbf{b}_i, i = 1, 2, 3$ = ith body-fixed unit vector
$b_i, i = 1, 2, 3$ = ith body-fixed coordinate axis
$\{C\}$ = 9 × 1 vector of acceleration difference terms
dt = time step increment
$\mathbf{F}_k$ = resultant force at arbitrary point k on limb segment
$\mathbf{g}$ = gravity acceleration
g = magnitude of gravity acceleration (9.80665m/s^2)
$g_i, i = 1, 2, 3$ = ith (body-fixed) component of gravity acceleration
II = central mass inertia dyadic along body-fixed axes
m = mass of leg
$\mathbf{M}_k$ = resultant moment at arbitrary point k on limb segment
$\mathbf{n}_i, i = 1, 2, 3$ = ith inertia-fixed unit vector
$n_i, i = 1, 2, 3$ = ith inertia-fixed coordinate axis
$\mathbf{P}$ = position vector from arbitrary point (0) to center of mass
$\mathbf{R}_i, i = 1, 2, 3, 4$ = position vector from arbitrary point (0) to accelerometer location i
$\mathbf{r}_i, i = 1, 2, 3, 4$ = position vector to accelerometer location i from center of mass
$\mathbf{r}_k$ = position vector to arbitrary point k from center of mass
$[S]$ = 9 × 9 matrix of position vectors
t = time
$\{X\}$ = 9 × 1 vector of angular parameters
$x_i, i = 1, 2, \ldots, 9$ = ith element of $\{X\}$ vector
α = angular acceleration of leg
$\alpha_i, i = 1, 2, 3$ = ith (body-fixed) component of acceleration
$\theta_i, i = 1, 2, 3$ = ith orientation angle
$\dot{\theta}_i, i = 1, 2, 3$ = ith orientation angle rate derivative
$\lambda_i, i = 1, 2, 3$ = position vector constant i
ω = angular velocity of leg
$\omega_i, i = 1, 2, 3$ = ith (body-fixed) component of angular velocity

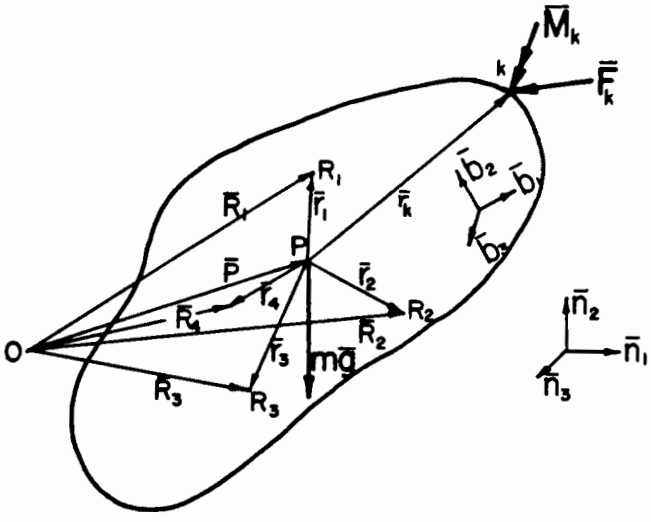

Fig. 2 Free-body diagram of limb segment

gage fixed to a cantilever beam carrying a small mass at its free end. When accelerated, this mass experiences a reaction force which is the vector sum of gravity and inertial forces. The reaction force which causes the strain in the beam is the product of mass and measured acceleration. The inertial force, by definition, is the negative of the product of mass and actual acceleration. Mathematically, after dividing through by mass,

$$-\mathbf{g} = \mathbf{a}_i^m - \mathbf{a}_i^a \tag{1}$$

where $\mathbf{g}$ is the gravity acceleration vector, $\mathbf{a}_i^m$ is the acceleration measured at accelerometer i, and $\mathbf{a}_i^a$ is the actual or true acceleration at accelerometer location i. Thus, a stationary accelerometer records an acceleration of one g unit in the direction of the earth's gravitation field; an accelerometer in free-fall records zero acceleration.

The use of four triaxial accelerometers to monitor rigid-body motion was described by Kane, et al. [13]. Consider a leg with accelerometers located at four noncoplanar points as modeled in the free-body diagram in Fig. 2. Since the accelerometers are attached to the leg, all accelerations are measured in the directions of body-fixed unit vectors ($\mathbf{b}_i$'s). The center of mass of the leg is located at point P. The origin of the body-fixed axes coincides with point P. (It is not drawn this way to avoid complicating the figure.) The weight vector, $m\mathbf{g}$, acts through point P in the local downward direction (the $-\mathbf{n}_3$ direction). Position vector $\mathbf{P}$ defines the location of the center of mass (point P) from an arbitrary point 0. The $\mathbf{r}_i$'s represent position vectors to the accelerometers from the center of mass (point P) and the $\mathbf{R}_i$'s designate position vectors from the arbitrary point 0 to the accelerometers. A resultant force, $\mathbf{F}_k$, and moment, $\mathbf{M}_k$, act at point k, which is regarded as the knee.

Kane, et al., derived the following expression for the acceleration of the center of mass, a,

$$\mathbf{a} = \frac{\lambda_1\mathbf{a}_1 + \lambda_2\mathbf{a}_2 + \lambda_3\mathbf{a}_3 - \mathbf{a}_4}{\lambda_1 + \lambda_2 + \lambda_3 - 1} \tag{2}$$

where $\mathbf{a}_i$ is the acceleration at location i and λ_i is a constant ($i = 1, \ldots, 4$). The constants λ_i are functions of the position vectors $\mathbf{r}_1, \ldots, \mathbf{r}_4$ and are derived by simple vector manipulations assuming that the accelerometers are mounted at four noncoplanar locations on the leg. The center of the mass of the leg, calculated by direct application of equation (2) with accelerometer measurements, contains components of acceleration due to gravity which are the same as the gravity components in the accelerometer measurements. This fact is used to calculate the angular velocity and angular acceleration of the leg. The fundamental kinematic relation for the acceleration $\mathbf{a}_i$ at location i on the leg is

$$\mathbf{a}_i = \mathbf{a} + \boldsymbol{\alpha}\times\mathbf{r}_i + \boldsymbol{\omega}\times(\boldsymbol{\omega}\times\mathbf{r}_i) \text{ for } i = 1, 2, 3, 4 \tag{3}$$

where $\mathbf{a}$ is the acceleration of the center of mass, $\boldsymbol{\alpha}$ and $\boldsymbol{\omega}$ are the angular acceleration and angular velocity of the leg, respectively, and $\mathbf{r}_i$ is defined as described in the foregoing. The unknowns in equation (3) are $\boldsymbol{\alpha}$ and $\boldsymbol{\omega}$. The accelerations $\mathbf{a}_i$ and $\mathbf{a}$ are not known explicitly due to the nature of the accelerometers. However, the quantity $(\mathbf{a}_i - \mathbf{a})$ is known and represents an actual acceleration difference since gravity is subtracted out. For convenience, the nonlinear kinematic relations of equation (3) are rewritten as a system of linear equations in terms of alternate angular quantities. Specifically, considering accelerometers $i = 1, 2, 3$, equation (3) is equivalent to the following matrix equation

$$[S]\{X\} = \{C\} \tag{4}$$

where $[S]$ is a 9×9 matrix of position vectors; $\{X\}$ is a 9-element vector of angular parameters; and $\{C\}$ is a 9-element vector of acceleration values. The elements of the $\{X\}$ vector are

$$\begin{aligned} x_1 &= \alpha_1 & x_2 &= \alpha_2 & x_3 &= \alpha_3 \\ x_4 &= \omega_2\omega_3 & x_5 &= \omega_3\omega_1 & x_6 &= \omega_1\omega_2 \\ x_7 &= \omega_2^2 + \omega_3^2 & x_8 &= \omega_3^2 + \omega_1^2 & x_9 &= \omega_1^2 + \omega_2^2. \end{aligned} \tag{5}$$

The elements of the $\{C\}$ vector are the components of three sets of acceleration differences, $(\mathbf{a}_i - \mathbf{a}) \cdot \mathbf{b}_j$, $j = 1, 2, 3$ for $i = 1, 2, 3$ which are known. The $[S]$ matrix is also known since the position vectors $\mathbf{r}_i$'s are known. The elements of the $\{X\}$ vector are determined by multiplying the inverted $[S]$ matrix by the $\{C\}$ vector. The $[S]$ matrix is nonsingular and thus can be inverted since the accelerometers are located at four noncoplanar points. This implies that any set of three accelerometers is noncolinear, the condition for nonsingular $[S]$. Equation (3) is equivalent to twelve scalar equations, although only nine need to be solved to determine the $\{X\}$ vector. Accelerometers $i = 1, 2, 3$ were used in the foregoing. Similarly, the other sets of three accelerometers can be used: $i = 1, 2, 4$, $i = 2, 3, 4$, and $i = 1, 3, 4$. For noise-free accelerometer measurements, these four combinations result in identical $\{X\}$ vectors. In actual implementation, to ensure that a maximum of information is extracted, equation (4) is solved four times using the four combinations of accelerometers and the resulting $\{X\}$ vectors are averaged.

This analysis generates the angular acceleration components (x_1, x_2, x_3) directly. The angular velocity components are not available due to lack of sign information. The magnitudes of the angular velocity components can be obtained by algebraic manipulation of $\{X\}$ vector elements. To determine the signs, an assumption concerning the sign of one of the angular velocity components must be imposed at time $t = 0$. Here, it is assumed that the angular velocity about the b_1 axis, ω_1, is negative at the initial time step. It follows then

$$\begin{aligned} \omega_1 &= -\tfrac{1}{2}\{(x_9 + 2|x_6|)^{1/2} \\ &\quad + (x_8 + 2|x_5|)^{1/2} - (x_7 + 2|x_4|)^{1/2}\} \\ \omega_2 &= -\frac{x_6}{2|x_6|}\{(x_9 + 2|x_6|)^{1/2} \\ &\quad + (x_7 + 2|x_4|)^{1/2} - (x_8 + 2|x_5|)^{1/2}\} \\ \omega_3 &= -\frac{x_5}{2|x_5|}\{(x_8 + 2|x_5|)^{1/2} \\ &\quad + (x_7 + 2|x_4|)^{1/2} - (x_9 + 2|x_6|)^{1/2}\}. \end{aligned} \tag{6}$$

Thus, the angular velocity and angular acceleration are

calculated directly from accelerometer measurements without knowledge of the orientation of the leg in space.

The orientation of the leg can now be determined. At the initial time step it is assumed that the lower leg rotates about a fixed point, the ankle, as suggested by Morris [10]. This occurs during the "foot-flat" period of the normal gait cycle. Selecting the starting point for the analysis during "foot-flat" reduces the degrees of freedom of the motion from six to three, since the leg can only rotate about a fixed point. The restriction of pure rotation implies that the actual acceleration at accelerometer location i is

$$\mathbf{a}_i^q = \overset{\alpha}{\Phi} \times \mathbf{R}_i + \omega \times (\omega \times \mathbf{R}_i) \tag{7}$$

where $\mathbf{R}_i$ is a position vector to accelerometer location i from point 0, the ankle. The negative of the gravity acceleration vector, $-\mathbf{g} = g\,\mathbf{n}_3$, can be expressed in terms of its components in body-fixed coordinates, g_1, g_2, g_3, by substituting equation (7) into (1). The components g_1, g_2, g_3, are the same at any accelerometer location, given noise-free accelerometer measurements. From the transformation between the body-fixed and the inertia-fixed unit vectors, g_1, g_2, and g_3 can be expressed in terms of g and of trigonometric functions of the orientation angles. Assuming that at time $t=0$, $\theta_3 = 0$ and $-90 \text{ deg} < \theta_i < +90 \text{ deg}$, $i = 1, 2$, direct manipulation yields the orientation angles θ_1 and θ_2

$$\theta_1 = \sin^{-1}(g_2/g) \tag{8}$$

$$\theta_2 = \sin^{-1}\left[\frac{-g_1/g}{(1-(g_2/g)^2)^{1/2}}\right]. \tag{9}$$

Thus, the initial orientation of the leg in space is completely determined from accelerometer measurements at four noncoplanar locations given four assumptions at time $t=0$: 1) the leg rotates about a fixed point; 2) the angular velocity about the b_1 axis is negative; 3) angular rotation about the b_1 and b_2 axes occurs only between -90 deg and $+90$ deg; and 4) the angular position about the b_3 axis (corresponding to the long axis of the leg) is set equal to zero. The initial orientation, together with accelerometer measurements at future time steps can then be used to find the subsequent orientation of the leg by integration.

The resultant force, F_k, and moment, M_k, which act at point k, the knee, can now be calculated by applying the principles of linear and angular momentum.

$$\mathbf{F}_k = m\mathbf{a} - m\mathbf{g} \tag{10}$$

$$\mathbf{M}_k = -(\mathrm{II}\omega \times \omega) + \mathrm{II}\alpha - \mathbf{r}_k \times \mathbf{F}_k. \tag{11}$$

The mass, m, and the centroidal mass inertial dyadic along body-fixed axes, II, are assumed known. The actual center of mass acceleration, $\mathbf{a}$, is calculated by substituting equation (7) into (2). In equation (11), $\mathrm{II}\omega$ and $\mathrm{II}\alpha$ represent matrix products [16]. Equations (10) and (11) are valid only during the swing phase of gait when no external forces (other than gravity) or moments act on the leg. To calculate the force and moment at the knee at the initial time step, these equations must include ground reaction forces and moments which are present since the leg is in the "foot-flat" phase of gait.

Analysis for Subsequent Time ($t>0$). The first objective of the analysis for the general time step is to calculate the orientation of the leg. Assuming small time step increments, current orientation angles, θ_1, θ_2, and θ_3, are found by numerical integration of the orientation angle rate derivative, $\dot{\theta}_i$, from the previous time step. These derivatives are easily related to the angular velocity components through a transformation matrix which consists of trigonometric functions of the orientation angles. This transformation is not valid when $\theta_2 = \pm 90$ deg for which $\dot{\theta}_1$ and $\dot{\theta}_3$ become infinite. However, this is not a serious restriction since this corresponds to a horizontal position of the leg.

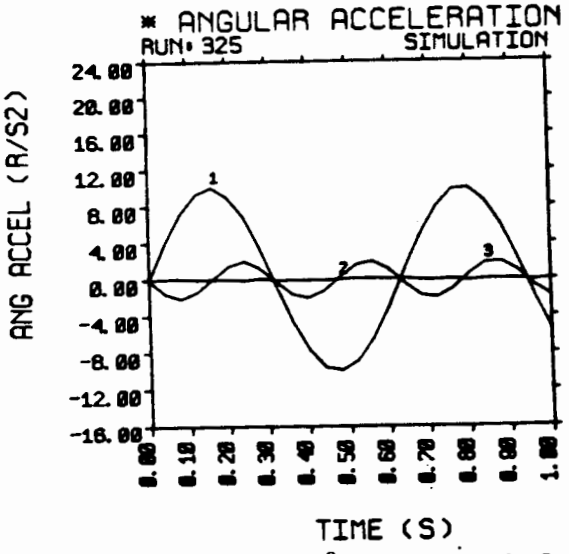

Fig. 3 Angular acceleration (rad/s^2) versus time (s) for 5 percent random-noise simulation

Given the current orientation of the leg, the gravity acceleration vector is expressed in body-fixed coordinates. Using a recast form of equation (1), the gravity acceleration vector is then eliminated from the accelerometry data to determine the actual acceleration at each accelerometer location. Direct application of equation (2) with these actual accelerations result in the actual center of mass acceleration. Equation (4) is then solved for the vector of angular parameters. (The angular parameters could have been calculated without recourse to actual accelerations.) The $[S]$ matrix is constant for all time steps since the accelerometer locations remain fixed on the leg; the $\{C\}$ vector changes for all time steps since it is a function of the (difference of) accelerations at the accelerometer locations and the center of the mass. As before, the angular acceleration components are the first three elements of the $\{X\}$ vector. To solve for the angular velocity components, ω_i's, the signs must first be determined. The sign of ω_1 is no longer assumed negative, but is determined for each time step by numerical integration of α_1. Similarly, the signs of ω_2 and ω_3 are determined by integration of α_2 and α_3, respectively. The angular velocity components are given by

$$\omega_i = (\operatorname{sgn} \omega_i)\,|\omega_i|, \; i = 1, 2, 3 \tag{12}$$

where $(\operatorname{sgn} \omega_i)$ refers to the sign of ω_i determined by integration of α_i and $|\omega_i|$ is the magnitude of ω_i calculated from equation (6).

Thus, the angular position, velocity and acceleration of the leg and the acceleration of the mass center are calculated for the current time step from accelerometry data. The resultant force and moment acting at the knee are calculated from equations (10) and (11). This completes the theoretical develoment for characterizing the dynamics of a leg during arbitrary motion given triaxial accelerometer measurements at four noncoplanar locations.

Simulation Studies

The validity of the theoretical approach was demonstrated with simulated three-dimensional rigid body motion involving both rotation and translation. The motion of a cylindrical rigid body (of mass 1.75 kg) possessing two large and equal diametral principal mass moments of inertia (0.16 kg-m^2) and a much smaller axial principal mass moment of inertia (0.0001 kg-m^2) was studied. The prescribed motion was large-amplitude, low-frequency sinusoidal oscillations about the

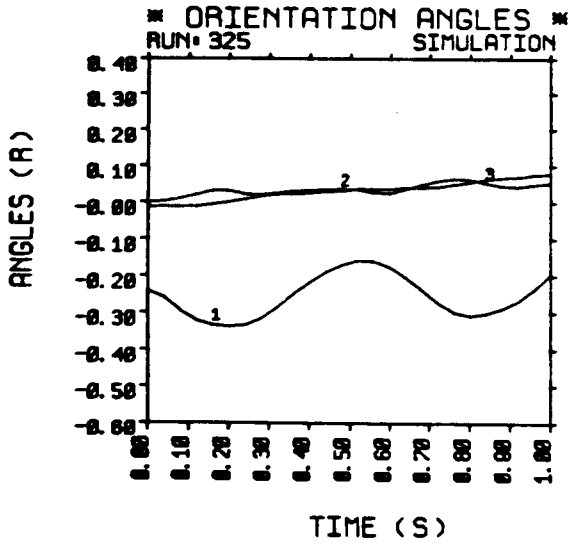

Fig. 4 Orientation angles (rad) versus time (s) for 5 percent random-noise simulation

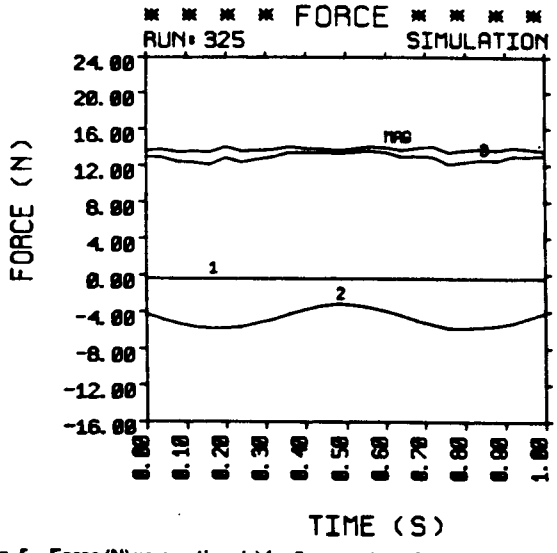

Fig. 5 Force (N) versus time (s) for 5 percent random-noise simulation

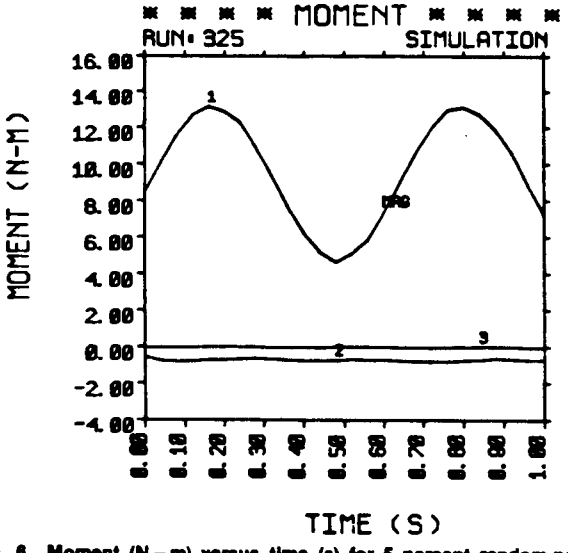

Fig. 6 Moment (N – m) versus time (s) for 5 percent random-noise simulation

body-fixed b_1 axis, and small amplitude, higher frequency sinusoidal oscillations about the b_3 axis.

Noise-free and 5 percent random-noise simulated data was calculated for one second of such motion at a sampling rate of 25 Hz. The random noise data was generated by multiplying the maximum value of the noise-free accelerometer data by 5 percent times a random number between zero and one and then randomly adding and subtracting it to the noise-free measurement at each time step. Since this procedure was performed for each axis of each accelerometer, use of the noisy data represents a severe test of the theoretical formulation.

A graph of the angular acceleration as a function of time obtained from noisy simulated data is shown in Fig. 3. This graph agrees with a graph of the angular acceleration history obtained from noise-free data. The method solves successfully for the angular acceleration from noisy accelerometry data since redundant data is available. At each time step, equation (4) is solved four times and the resulting $\{X\}$ vector elements are averaged.

The angular velocity is calculated by algebraic manipulation of the accelerometer measurements and position vector information. The angular velocity history based on noise-free data is identical to that obtained by numerical integration of the angular acceleration, using the appropriate initial conditions (i.e., those calculated in the initial conditions analysis). With noisy data, the angular velocity does not agree as well with the integration of the angular acceleration. The angular velocity about the b_2 axis assumes nonzero values, and the angular velocity about the b_3 axis no longer reflects a small amplitude, high frequency oscillation. This can be explained by comparing the relative magnitudes of the terms in the fundamental kinematic relation, equation (3). During most of the prescribed motion, the magnitude of the tangential acceleration term, involving the cross product of the angular acceleration and a position vector, is much larger than the magnitude of the centrifugal acceleration term, composed of a triple cross product of the angular velocity and a position vector. Thus, the centrifugal acceleration term undergoes a much larger percent change than does the tangential acceleration term. With noisy data, the larger percent error in the centrifugal acceleration term is responsible for the error in the angular velocity, while the smaller percent error in the tangential acceleration term allows for successful calculation of the angular acceleration.

A graph of the angular orientation obtained from 5 percent random noise data is shown in Fig. 4. The angles θ_2 and θ_3 drift after one second of simulated motion. The orientation angles are found by integration of the orientation angle rates, which are calculated from noisy angular velocity components.

Most importantly, the simulation studies demonstrate the ability of the method to self-generate the initial spatial orientation of the rigid-body from accelerometer measurements. For the noise-free run, the initial orientation angles θ_1 and θ_2 used to calculate the simulated data (at $t = 0$) agree with the angles calculated by the analysis to seven significant figures: $\theta_1 = -0.25$, $\theta_2 = \theta_3 = 0.00$ rad. With noisy data, the method maintains its ability to self-generate the initial orientation angles. It calculated $\theta_1 = -0.245$, $\theta_2 = -0.011$, and $\theta_3 = 0.001$ rad.

The strength of the technique is ultimately based on its ability to successfully solve for the resultant force and moment which must have been imposed to execute the motion. Figures 5 and 6 display the force and moment graphs, respectively, for the random noise runs. Each graph shows the magnitude as well as the three vector components. For the noisy run, the calculations are based on the unsmoothed

A controlled verification experiment was performed by analyzing the motion of a two-dimensional compound pendulum, shown schematically in Fig. 7 with accelerometer locations and body-fixed axes marked. Four triaxial accelerometers were used in this study, each weighing 0.5g and measuring 1 cm^3 (Entran Devices EGAL 3-125-5D). The sensitivity of these transducers was on the order of 7 mV/g, with a maximum output of ±35 mV in the linear response range (± 5g). Cross axis sensitivity was specified to be 3 percent or less. For signal conditioning, a 12-channel Vishay Instruments 2100 System was used to provide an excitation voltage to the bridge circuit of each axis of each accelerometer and to amplify the output voltage. A Honeywell 1858 Multichannel Visicorder provided a permanent record of the acceleration data. Automatic data recording was accomplished using a DEC PDP 11/V03 minicomputer system in conjunction with an analog-to-digital (A/D) converter (Data Translation Model DT2762) and real-time clock (DEC KWV11).

Experimental accelerometry data was acquired once the pendulum was set in motion. To satisfy an assumption of the analysis, data acquisition was initiated when the angular velocity about the b_1 axis was negative. The period of the pendulum was 1.25 s.

Verification of the theoretical formulation involved comparing calculated angular parameters with those predicted by an independent analysis which solved the dynamic equations of motion of a compound pendulum executing large rotations [17]. The pendulum analysis [17] represented an approximation since it did not include frictional damping. Since a two-dimensional pendulum was used, only b_1 components of angular acceleration, velocity, and orientation existed. The results of the accelerometry calculation gave a b_1 component of angular acceleration which agreed with that determined by the pendulum analysis and zero b_2 and b_3 components. In comparing the results of the accelerometry and pendulum calculations, agreement was also obtained for the b_1 component of angular velocity. However, the accelerometry method incorrectly predicted nonzero b_2 and b_3 components, with magnitudes approximately 5 percent of the maximum value of the b_1 component. As discussed earlier, the calculation of angular velocity is more sensitive to noisy data than the calculation of angular acceleration.

Three independent curves of the angular position versus time are shown in Fig. 8. The results of the accelerometry and pendulum calculations appear, as well as the angular position as measured by a Rotary Variable Differential Transformer connected to the pendulum axle. The curves representing the pendulum calculation and the RVDT output show close agreement, whereas the curve representing the results of the accelerometry calculation show marked deviation. According to the accelerometry results, the pendulum started at 37 deg (0.65 rad) at the outset of its swing, but swung to −55 deg (−0.96 rad) on the extreme opposite side. This result is impossible in the absence of externally applied forces other than gravity. The angular position is found by integration and, therefore, depends on the results of the previous time step. Any error in calculation at a particular time step will then become part of the integration and accumulate with time.

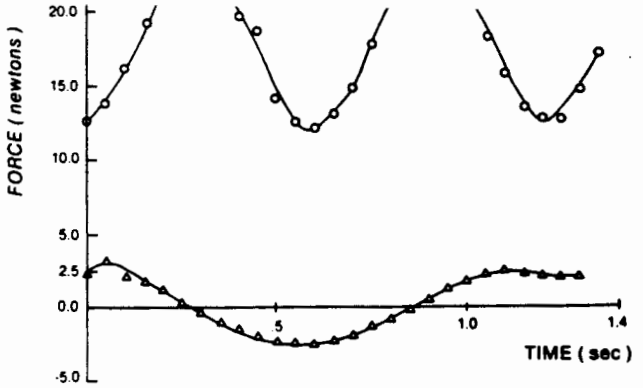

Fig. 9 b_2 and b_3 components of force (N) versus time (s) calculated by accelerometry analysis

Despite this problem with angular position, these results confirm the validity of accelerometry as a viable technique to study the dynamics of leg motion. It is the angular velocity and acceleration which are required to find force and moment information. Figure 9 is a plot of force as a function of time. The centrifugal force (b_3) is maximum when the pendulum is vertical and minimum at the endpoints. Tangential forces (b_2) are most positive at the starting position and most negative at the opposite endpoint due to the large contribution by the earth's gravitational field. Moment (b_1 component) versus time is displayed in Fig. 10.

Discussion

The highly insular nature of the pendulum system required

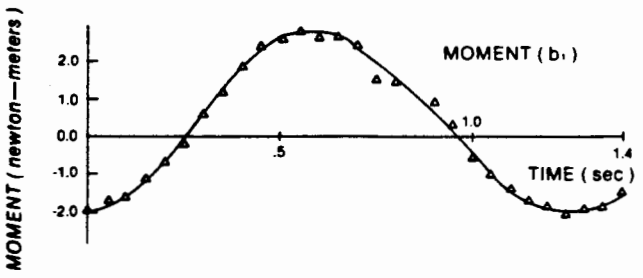

Fig. 10 b_1 component of moment (N – m) versus time (s) calculated by accelerometry analysis

to obtain verification has exposed many of the severe limitations which must be surmounted before multiaxial accelerometry can be utilized as a tool to study the lower leg during gait. Accelerations of points on the leg during the swing phase of the gait cycle are on the order of several g-units. The accelerometers employed in the pendulum experiment operate in the ±5-g range and it might appear that they would be suitable for swing-phase gait studies. However, the accelerometers are quite sensitive, capable of measuring accelerations that are fractions of g-units. Consequently, when functioning in the laboratory environment, the accelerometers are sensitive to vibrations originating from sources such as heavy equipment in the building. This high sensitivity to vibration has the effect of introducing artifacts into the data. The possibility exists of filtering these artifacts; however, a careful frequency analysis of the signals must be performed to insure that no desired information is lost. An advantage of the accelerometry technique, versus the cinematographic approach, is that analog signals are available for filtering.

The large accelerations and impulse effects at "heel-strike" would have a devastating effect on miniature accelerometers attached to the shank. In particular, at "heel-strike" these accelerometers would be permanently offset rendering further signals meaningless. Even with recent promising results for skin-mounted miniature accelerometers, soft tissue vibration will introduce unwanted noise in the data. Ziegert and Lewis [18], for instance, demonstrated that a 1.5-g skin-mounted accelerometer on the shank showed nearly identical output to tibia acceleration. Motor tremors of the body and shank during gait will undoubtedly add a component of noise. It appears that these difficulties cannot be overcome with present transducer design, and that a major thrust of future work in gait analysis by accelerometry will lie in the redesign of the accelerometers and in the development of efficient coupling procedures.

Conclusions

The accelerometry method presented here employs body-fixed multiaxial accelerometers and models the leg as a rigid body. A significant contribution of the theoretical development is the self-generating character of the initial angular orientation of the leg. This necessary information can be calculated since: 1) the accelerometer measurements contain gravity vector components; and 2) it is assumed that the leg executes pure rotation about a known fixed point at the initial time step. Body-fixed linear accelerometer measurements are used to calculate the leg's angular acceleration and velocity. Assuming accurate estimates of segment mass inertial properties, the angular acceleration and velocity can then be used to determine the resultant force and moment at the knee.

The present investigation provides an alternative approach based on direct measurements of acceleration using multiaxial accelerometry to study complex three-dimensional leg motions during gait. The approach avoids the errors inherent in the differentiation of displacement data and allows for the direct calculation of resultant forces and moments applied to the leg at the knee. Results of validation experiments using both artificial and experimental data demonstrate that the method is theoretically correct, but that presently it taxes available instrumentation and requires further development before it can be considered as a clinical tool.

Acknowledgments

This work was supported in part by research grants AM 20135 and 5T32GM07301 from the National Institutes of Health. We thank Dr. A. Soler, Professor of Mechanical Engineering at the University of Pennsylvania for his many helpful discussions. We would also like to acknowledge the technical support of Mr. S. Richardson. Mr. G. McKenna helped with data transfer from the minicomputer to the DEC-10 system. We are also grateful for the support of the staff of the University of Pennsylvania Medical School Computer Facility.

References

1 Pezzack, J. C., Norman, R. W., and Winter, D. A., "An Assessment of Derivative Determining Techniques Used for Motion Analysis," *Journal of Biomechanics*, Vol. 10, 1977, pp. 377-382.

2 Soudan, K., and Dierckx, P., "Calculation of Derivatives and Fourier Coefficients of Human Motion Data, While Using Spline Functions," *Journal of Biomechanics*, Vol. 12, 1979, pp. 21-26.

3 Zernicke, R. F., Caldwell, G., and Roberts, E. M., "Fitting Biomechanical Data with Cubic Spline Functions," *Research Quarterly*, Vol. 47, No. 1, 1976, pp. 9-18.

4 Rydell, N. W., "Forces in the Hip Joint," *Biomechanics and Related Bioengineering Topics*, ed., R. M. Kenedi, Pergamon Press, London, 1965.

5 Brown, R., Burstein, A. H., and Frankel, V. H., "Telemetering *In-Vivo* Loads from Nail Plate Implants," *Journal of Biomechanics*, Vol. 15, 1982, pp. 815-823.

6 Brown, R., and Hipel, K. H., personal communication, 1978.

7 Kilvington, M. and Goodman, R. M. F., "*In-Vivo* Hip Joint Forces Recorded on a Strain Gaged (English) Prosthesis Using an Implanted Transmitter," *Engineering in Medicine*, Vol. 10, 1981, pp. 175-187.

8 Chao, E. Y. S., "Hip Biomechanical Function," *NIH Consensus Development Conference on Total Hip Joint Replacement Proceedings*, 1982, pp. 31-37.

9 Gage, H., "Accelerographic Analysis of Human Gait," ASME Technical Report 64-WA/HUF-8, 1964, pp. 1-12.

10 Smidt, G. L., Arora, J. S., and Johnston, J. C., "Accelerographic Analysis of Several Types of Walking," *American Journal of Physical Medicine*, Vol. 50, No. 6, 1971, pp. 285-300.

11 Robinson, J. L., Smidt, G. L., and Arora, J. S., "Accelerographic, Temporal, and Distance Gait Factors in Below-Knee Amputees," *Physical Therapy*, Vol. 58, No. 8, 1977, pp. 898-904.

12 Morris, J. R., "Accelerometry—A Technique for the Measurement of Human Body Movements," *Journal of Biomechanics*, Vol. 6, 1973, pp. 729-736.

13 Kane, T. R., Hayes, W. C., and Priest, J. D., "Experimental Determination of Forces Exerted in Tennis Play," *Biomechanics IV*, University Park Press, Baltimore, 1974, pp. 284-290.

14 Padgaonkar, A. J., Krieger, K. W., and King, A. I., "Measurement of Angular Acceleration of a Rigid Body Using Linear Accelerometers," ASME *Journal of Applied Mechanics*, Vol. 42, 1975, pp. 552-556.

15 Mital, N. K., and King, A. I., "Computation of Rigid-Body Rotation in Three-Dimensional Space From Body-Fixed Linear Acceleration Measurements," ASME *Journal of Applied Mechanics*, Vol. 46, 1979, pp. 925-930.

16 Kane, T. R., *Dynamics*, Holt, Rinehart, and Winston, New York, 1968.

17 Feldman, J. M., "Real-Time Processing and Multiaxial Accelerometry: A New Approach to Clinical Gait Analysis," M.S. thesis, University of Pennsylvania, 1980.

18 Ziegert, J. C., and Lewis, J. L., "The Effect of Soft Tissue on Measurements of Vibrational Bone Motion by Skin-Mounted Accelerometers," ASME JOURNAL OF BIOMECHANICAL ENGINEERING, Vol. 101, 1979, pp. 218-220.